ELSEVIER

Polymer 42 (2001) 3087–3093

polymer

www.elsevier.nl/locate/polymer

Miscibility in blends of poly (4-vinylpyridine)/poly (4-vinylphenol) as studied by ^{13}C solid-state NMR

Jian Wang[a], Man Ken Cheung[b], Yongli Mi[a,*]

[a]Department of Chemical Engineering, The Hong Kong University of Science and Technology, Clear Water Bay, Kowloon, Hong Kong, People's Republic of China

[b]Department of Applied Biology and Chemical Technology, The Hong Kong Polytechnic University, Hung Hom, Kowloon, Hong Kong, People's Republic of China

Received 11 July 2000; received in revised form 21 August 2000; accepted 22 August 2000

Abstract

The miscibility of poly (4-vinylpyridine) (P4VP) with poly (4-vinylphenol) (PVPh) blends was investigated over a wide range of compositions by differential scanning calorimeter (DSC), Fourier transform infrared spectroscopy (FTIR), and high-resolution solid-state nuclear magnetic resonance (NMR) spectroscopy. DSC results show that the T_gs of the P4VP/PVPh blends are much higher than those of the calculated weight-average values. The proton spin–lattice relaxation times in the laboratory frame, $T_1(H)$, and the rotating frame, $T_{1\rho}(H)$, were studied as a function of blend composition. $T_1(H)$ and $T_{1\rho}(H)$ results demonstrate that the spin diffusion can completely average out the entire relaxation process. It was also found that the intimate mixing of the polymer blends restricts the local chain mobility. © 2001 Elsevier Science Ltd. All rights reserved.

Keywords: Poly (4-vinylpyridine); Poly (4-vinylphenol); Polymer blends

---

1. Introduction

Polymer blends have been of great interest to materials scientists because of the improved and modified properties over the individual constituent polymers, for blending has the effect of toughening and strengthening for engineering applications. It was already reported that polymer blending can lead to functional polymeric materials that have desired electrical conductivity and magnetic properties [1,2]. Since the physical properties of polymer blends are strongly influenced by blending conditions and processes, there is a growing interest in studying miscibility and phase behavior of polymer blends.

Many studies of the polymer blends by differential scanning calorimetry (DSC), Fourier transform infrared spectroscopy (FTIR), transmission electron microscopy (TEM), and light scattering, have been reported [3–6]. DSC is one of the most widely used techniques for evaluating miscibility on a scale of 100–300 Å in terms of cooperative motion of polymer segments around the glass transition temperature (T_g) [6,7]. However, if the glass transition temperatures of the two constituent components are too close, i.e. the difference in T_g is less than 10°C, it is impossible to identify whether there are two or one T_g in the blend. Therefore, the miscibility cannot be judged for such blending systems. IR spectroscopy is also useful for the study of polymer miscibility because the interactions between the components can be detected by observing the change of the intensity, frequency, and the width of absorption bands for certain stretching bonds.

^{13}C solid-state nuclear magnetic resonance (NMR) has proven to be a very useful method for investigating not only the molecular motion but also the scale of miscibility. NMR parameters are sensitive to the effects of spin diffusion and can monitor variations among discrete structural entities [8,9]. ^{13}C chemical shifts and line shapes in the cross-polarization (CP)/magic angle spinning (MAS)/dipolar decoupling (DD) NMR spectra identify chemical environments of carbons in the blends, and changes are usually indicative of the specific interactions between the components [10–12].

Certain proton relaxation times are sensitive to the domain size of polymer blends through the process of spin diffusion. Two useful proton spin-relaxation times that can be obtained from ^{13}C solid-state NMR are the spin–lattice relaxation time in the laboratory frame, $T_1(H)$ and in the rotating frame, $T_{1\rho}(H)$, respectively. Proton spin diffusion is

---

* Corresponding author. Fax: +852-3580054.
E-mail address: keymix@usthk.ust.hk (Y. Mi).

0032-3861/01/$ - see front matter © 2001 Elsevier Science Ltd. All rights reserved.
PII: S0032-3861(00)00643-1

not a physical movement of protons, but is rather a transfer of spin energy by successive energy-conserving spin flips between a more magnetized region and a less magnetized region [9,15–17]. The spin diffusion process may be modeled as Fickian diffusion. Inter-domain spin diffusion in polymer blends may be detected directly by ^{1}H CRAMPS (combination of rotation and multiple pulse spectroscopy), ^{1}H WISE (wide-line separation), and Goldman–Shen experiments, or indirectly by its effects on the proton relaxation times, $T_1(H)$ and $T_{1\rho}(H)$. $T_1(H)$ is measured at specific protonated carbon sites by first having the protons go through inversion-recovery (IR) before CP to ^{13}C. $T_{1\rho}(H)$ is measured by monitoring the cross-polarized ^{13}C intensity after a variable proton spin-lock time. The ^{13}C intensity is a function of the varying delay time, and it yields $T_1(H)$ or $T_{1\rho}(H)$ as the exponential time constant. When phase domain sites are of the order of 10 nm or less, inter-domain spin diffusion averages out the $T_1(H)$ of each different domain to one effective $T_1(H)$ value. When the domains are greater than 50 nm, multiple $T_1(H)$ and $T_{1\rho}(H)$ are often observed. During the period of $T_{1\rho}(H)$ relaxation, proton spin diffusion covers a distance of about 3 nm. If one effective $T_{1\rho}(H)$ is observed and the intrinsic $T_{1\rho}(H)$s of the segments domains are different, it means that the domain size is below 1–3 nm [13–18].

In this study, the polymer blends of poly (4-vinylpyridine) (P4VP) with poly (4-vinylphenol) (PVPh) were studied. PVPh has stronger proton donor groups and it has been reported that PVPh is miscible with polymers such as polyacrylates [19], polymethacrylates [20,21], polyesters [19,22–24]. P4VP has similar structure to that of PVPh, in which the phenolic aromatic ring is replaced with a pyridine ring. The nitrogen atom on the pyridine ring of P4VP can act as a proton acceptor. De Meftahi and Fréchet have previously studied the miscibility of P4VP and PVPh blends by DSC measurements [25], and they found that polymer complexes could form when pyridine and methanol were used as the solvents for the sample preparation. The glass transition temperatures of the complexes are much higher than those of the pure components, which indicates strong hydrogen bonding exists between P4VP and PVPh. The objective of this study is to investigate the specific interaction, microstructure and homogeneity of the P4VP/PVPh blends by high-resolution solid-state ^{13}C NMR, DSC and, FTIR.

2. Experimental

2.1. Materials and the sample preparation

The polymers used in this study, P4VP and PVPh were purchased from Polysciences, Inc in Warrington, PA, USA. The average molecular weights are 150,000–200,000 and 22,000, respectively. The P4VP/PVPh blends were prepared by solution casting from *N*, *N*-dimethylformamide (DMF) by slow evaporation at 60°C for 1 week; the residual solvent was removed under vacuum at 80°C for 4 weeks.

2.2. Differential scanning calorimeter

The calorimetric measurements were carried out on a Perkin–Elmer Pyris-1 differential scanning calorimeter under a dry nitrogen atmosphere. The instrument was calibrated with indium and zinc standards for lower and high temperature regions, respectively. The midpoint of the slope change of the heat capacity of the second heating scan was taken as glass transition temperature (T_g). A heating rate of 20°C min^{-1} was used.

2.3. Fourier transform infrared spectroscopy

A Perkin–Elmer PC-16 spectrometer was used to study hydrogen-bonding interactions. Thin films of the blends were cast on NaCl windows from 0.5% (w/v) DMF solutions. After most solvent evaporated at room temperature, the films were transferred to a vacuum oven and were kept at 80°C for 2 weeks to remove the residual solvent. All the spectra were recorded at room temperature. A minimum of 32 scans at a resolution of 2 cm^{-1} was signal averaged. The films used in this study were sufficiently thin to obey the Beer–Lambert law.

2.4. Solid state NMR

High-resolution solid-state NMR experiments were carried out at ambient temperature (27°C) on a JEOL JNM-EX400 FT NMR spectrometer at the resonance frequencies of 399.65 MHz for Proton and 100.40 MHz for carbon-13. High-resolution ^{13}C NMR spectra were obtained using the CP/MAS together with the high-power DD. The 90° pulse width of 5.5 μs was employed with free induction decay (FID) signal accumulation. The CP Hartmann–Hahn contact time was set at 1.0 ms for all experiments, which was demonstrated to be a suitable time for detecting CP/MAS/DD NMR spectra for both the pure components and the blends. The rate of MAS was 5.0–5.4 kHz for measuring ^{13}C spectra and relaxation times. Total sideband suppression (TOSS) was used for suppressing the spinning side bands. The ^{13}C chemical shifts were calibrated by taking the ^{13}C chemical shift of the methine carbon of solid adamantine (29.5 ppm relative to TMS) as an external reference.

The proton spin–lattice relaxation time in the laboratory frames, $T_1(H)$, were measured by monitoring the decay of specific carbon peak intensities after a $\pi-\tau-\pi/2$ IR pulse sequence followed by CP using the IR method. The proton spin–lattice relaxation times in the rotating frame, $T_{1\rho}(H)$, were determined by observing the carbon signal intensities with a ^{1}H matched spin-lock pulse sequence prior to CP (spin-locking method).

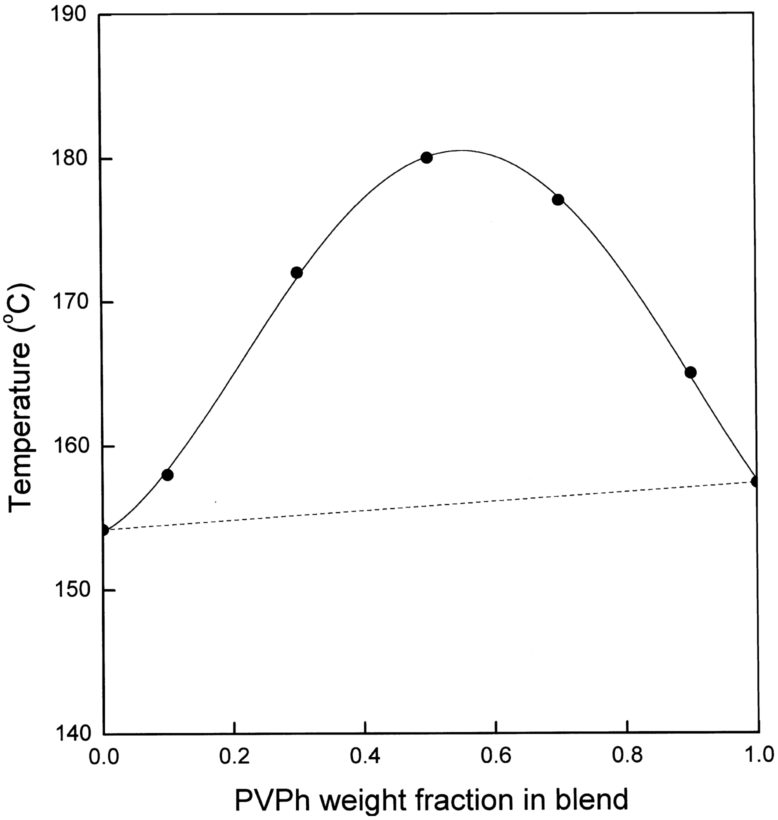

Fig. 1. Plot of glass transition temperatures for P4VP/PVPh blends versus weight fraction of PVPh. Solid dots (●) are experimental values.

3. Result and discussion

3.1. Differential scanning calorimetry

Studies have been reported of the effect of the solvent used in preparing polymer blends on the miscibility and the phase structures of the blends [26,27]. When mixing methanol solutions of P4VP and PVPh at 1:1 molar ratio, polymer complex was obtained on precipitation [25]. Complex formation was attributed to the strong hydrogen bonding between the two polymers and the weak interaction between the polymers and the solvent. DMF was used as the solvent in this study since DMF is a polar solvent that has strong interaction with the polymers that have polar groups. As a result, precipitation from solution in preparing P4VP and PVPh blends was avoided. All the P4VP/PVPh blends were subjected to DSC measurements. The T_g data were plotted vs. blend composition in Fig. 1. For all different compositions, the T_gs are higher than those of the calculated weight-averaged values. More interestingly, the maximum T_g appears at around 50-wt% composition. We believe that, since the molar mass of the repeating units of P4VP and PVPh are very close, the blend with 1:1 molar ratio should have the maximum number of the coupling pairs of the hydrogen bonds thus formed, and the highest glass transition temperature should be observed. The large positive deviation from the calculated values indicates that, during solvent evaporation, polymer complex was formed, for it is well known that the glass transition temperature of polymer complexes is significantly higher than those of the pure constituent components [25,26].

3.2. Fourier transform infrared spectroscopy

Fig. 2 shows the infrared spectra of the P4VP/PVPh blends in the hydroxyl stretching region at room temperature. Two vibration bands related to ‘free’ and intra-associated O–H groups appear in pure PVPh in curve A at 3510 and 3353 cm^{-1}, respectively. As the P4VP content in the blends increases, the intensity of the free hydroxyl band at 3510 cm^{-1} decreases. Furthermore, the center of the broad hydrogen bonded band shifts from 3353 to 3151 cm^{-1} when the content of P4VP increases to 70-wt%. The high frequency shift (202 cm^{-1}) reveals that the inter-molecular hydrogen bonding of P4VP/PVPh blends is stronger than the intra-molecular hydrogen bonding of PVPh.

Fig. 3 shows the infrared spectra between 1350 and 1100 cm^{-1}. There is a broad and strong absorption peak at 1232 cm^{-1} in curve A that corresponds to the stretching vibration of Ar–O bonds of PVPh. This peak also shifts to high frequency with the addition of P4VP. A total shift of 17 cm^{-1} can be observed when the content of P4VP increases to 70%. The higher frequency shift also indicates that stronger inter-molecular interactions exist in the blends.

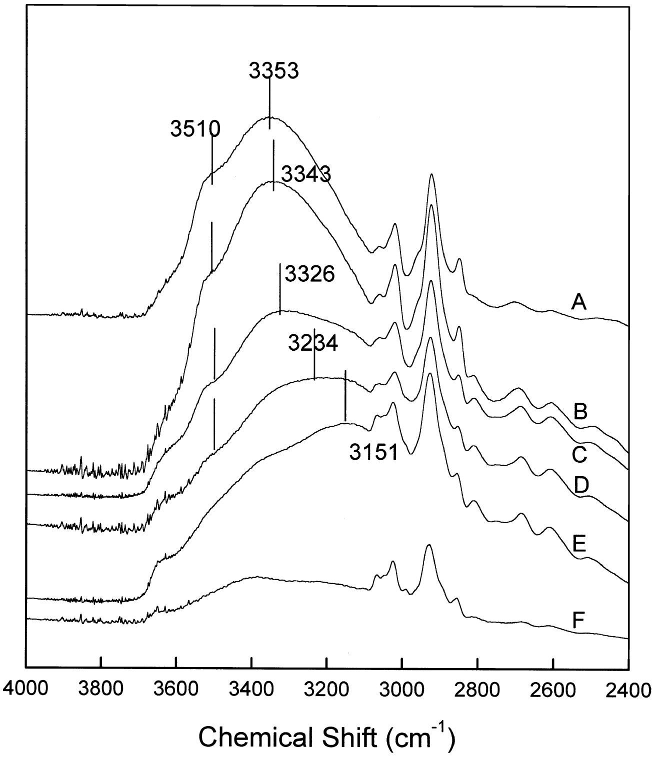

Fig. 2. FTIR spectra in the hydroxyl region of the P4VP/PVPh blends: (A) 100; (B) 90; (C) 70; (D) 50; (E) 30 and (F) 10 wt% PVPh.

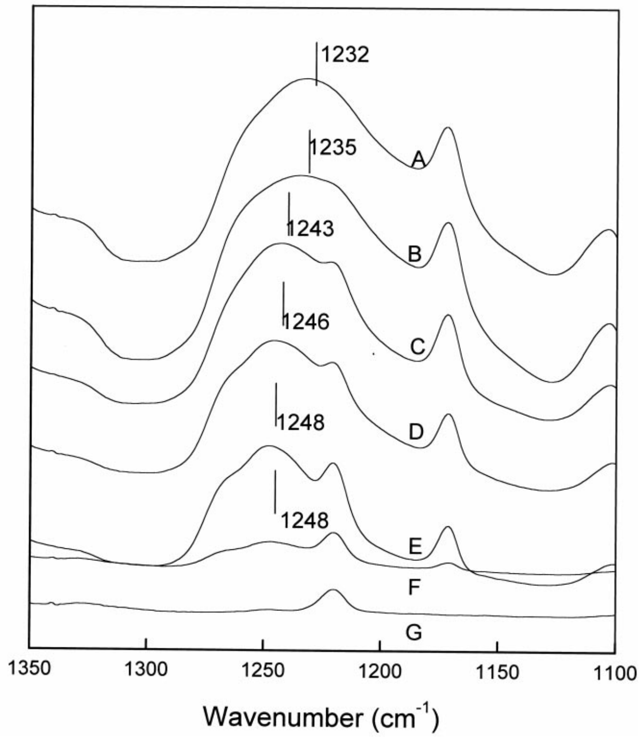

Fig. 3. FTIR spectra in the vibration region of PVPh Ar–O bonds of the P4VP/PVPh blends: (A) 100; (B) 90; (C) 70; (D) 50; (E) 30; (F) 10 and (G) 0 wt% PVPh.

3.3. ^{13}C CP/MAS/DD solid-state NMR spectra

The ^{13}C CP/MAS/DD spectra of P4VP, PVPh and their blends are shown in Fig. 4. Assignments of resonance line of P4VP and PVPh were made by the reference to the previous reports and were shown in Table 1 [28–30]. All other peaks in the ^{13}C NMR spectra are due to spinning side bands associated with the aromatic resonance of P4VP and PVPh.

Table 1
Assignment of ^{13}C CP/MAS spectra of P4VP and PVPh at 300 K

Compound	Structure	Carbon	Assignment (ppm)
P4VP	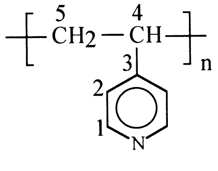	1,3 2 4,5	150.7 123.4 40.3
PVPh	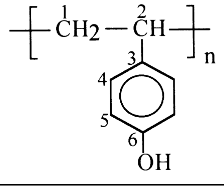	1,2 3 4 5 6	40.3 138.5 128.2 116.2 153.8

3.4. Proton spin–lattice relaxation time

To obtain more detailed information about the scale of miscibility and phase structure of the P4VP/PVPh blends, dynamic relaxation experiments were conducted, which include the measurements of the spin–lattice relaxation time in the laboratory frame, $T_1(H)$, and in the rotating frame, $T_{1\rho}(H)$. In $T_1(H)$ experiment, peak intensities of P4VP, PVPh, and their blends change exponentially as a function of delay time (τ) and the $T_1(H)$ values can be calculated using the following equation

$$\ln[(M_e - M_\tau)/(2M_e)] = -\tau/T_1(H) \qquad (1)$$

where $T_1(H)$ is the proton spin–lattice time in the laboratory frame, τ the delay time used in the experiment, M_τ the corresponding resonance intensity and M_e the intensity of the resonance at $\tau \geq 5T_1(H)$. Fig. 5 shows the plots of $\ln[(M_e - M_\tau)/(2M_e)]$ versus spin-locking time, τ, for selected carbons of PVPh (C-3) and P4VP/PVPh 50/50 blends. The experimental data can be fit to a single exponential decay function, and from the slopes of the plots, $T_1(H)$ values can be obtained. It is found that the single $T_1(H)$ decays are obtained for all blends, which indicates that fast spin diffusion occurred among all protons in these blends in the entire relaxation process. In addition, it is also found that the $T_1(H)$ values of the blends are shorter than those of the pure components, which indicates that the intermolecular interactions are stronger than the intra-molecular self-associations. This specific interaction is analyzed to be hydrogen bonding between the nitrogen in the pyridine ring of P4VP and the hydroxyl groups in PVPh as discussed below.

^{14}N is a quadrupolar nucleus with a spin number of 1, and a natural abundance of 99.63%. The $T_1(H)$ for pure P4VP is about 1.6 s, and ^{14}N is symmetrical in the pyridine ring (Table 2). The bonding environment of ^{14}N is changed due to hydrogen bonding with the hydroxyl-substituted carbon of PVPh after blending, so that ^{14}N is no longer symmetrical and its electric field gradient is no longer zero. Since the electric field gradient is randomly modulated by the molecular motion and by the bonding environment, the fluctuating electric field gradient provides a pathway for spin–lattice relaxation, and $T_1(H)$ relaxation of the protons becomes much more efficient by coupling to ^{14}N. Therefore, it can be concluded that the blends are homogeneous on the scale where the spin diffusion occurs within the times $T_1(H)$s. The mixing scale can be estimated using the one-dimensional diffusion equation for the average diffusive path length [31–33]:

$$\langle L^2 \rangle = (6DT_i) \qquad (2)$$

where D is the spin-diffusion coefficient which depends on the average proton to proton distance as well as dipolar interaction. It has a typical value of the order of $4\text{–}6 \times 10^{-16}\ \mathrm{m^2\,s^{-1}}$. T_i is the relaxation time, $T_1(H)$ or $T_{1\rho}(H)$, according to the relaxation experiment. On the basis of $T_1(H)$, it is believed that the two polymers are intimately mixed on a scale of less than 60–80 nm. Since

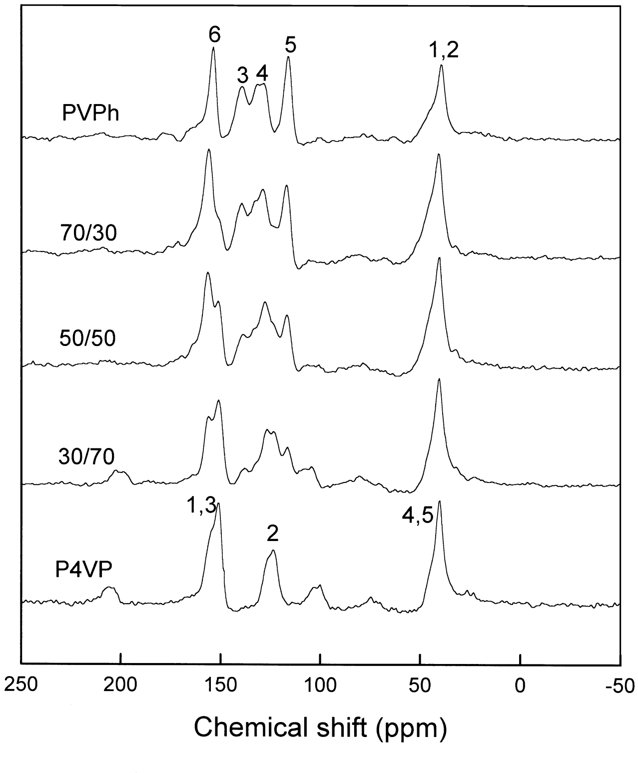

Fig. 4. ^{13}C CP/MAS/DD spectra of the P4VP/PVPh blends.

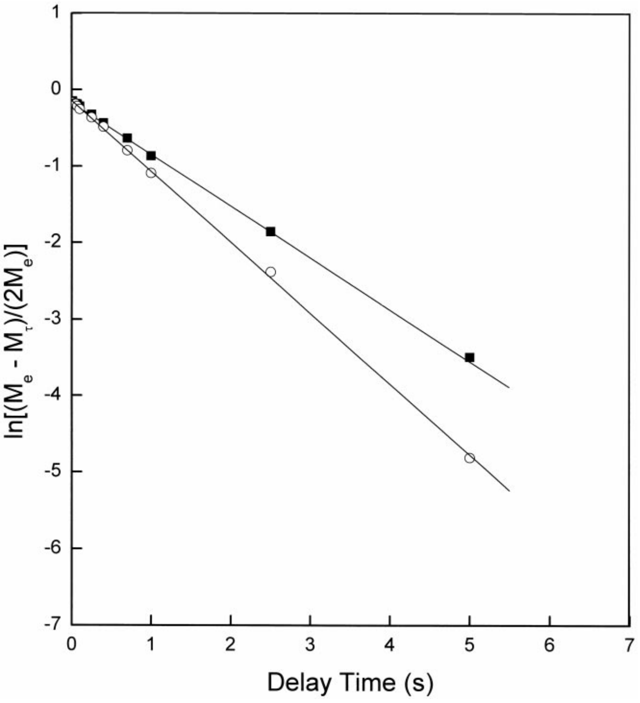

Fig. 5. Logarithmic plot of the peak intensities vs delay time of $T_1(H)$ for the selected carbons of PVPh (C-3). (■) PVPh (○) P4VP/PVPh 50/50.

Table 2
$T_1(H)$ values (s) of P4VP/PVPh blends at 300 K (the accuracy of the measurements is ±5%)

Composition (P4VP wt%)	P4VP C-4,5	PVPh C-5
0	–	1.32
30	1.08	0.94
50	1.10	0.97
70	1.20	0.93
100	1.55	–

Table 3
$T_{1\rho} >$ (H) values (ms) of P4VP/PVPh blends at 300 K (the accuracy of the measurements is ±5%)

Composition (P4VP wt%)	P4VP C-4,5	PVPh C-5
0	–	6.80
30	8.69	9.10
50	8.40	9.40
70	7.80	10.71
100	6.79	–

such mixing level reflects the sum of domain A plus domain B of the blends, the domain size of a constituent domain is less than 40 nm.

The spin–lattice relaxation time in the rotating frame $T_{1\rho}(H)$ was measured to examine homogeneity of the P4VP/PVPh blends at the molecular level. In this measurement, the intensities of carbon peaks of P4VP, PVPh and their blends display single exponential decays as a function of delay time, and the $T_{1\rho}(H)$ values were calculated according to the exponential function model:

$$M_\tau = M_0 \exp[-\tau/T_{1\rho}(H)] \tag{3}$$

Rearranging Eq. (4) and taking the natural logarithm, we have:

$$\ln(M_\tau/M_0) = -\tau/T_{1\rho}(H) \tag{4}$$

Fig. 6 shows the plots of $\ln(M_\tau/M_0)$ versus spin-locking time, τ, for selected carbons of PVPh (C-3) and P4VP/PVPh 50/50 blends. It is found that the experimental data can be fit to a single exponential decay function, and the slope gives the $T_{1\rho}(H)$ value. Referring to Table 3, one finds that the $T_{1\rho}(H)$ values of the P4VP/PVPh blends (30/70, 50/50, 70/30) are longer than those of the two pure components. It is known that the $T_{1\rho}(H)$ relaxation process is not due to the quadrupole frequency because $T_{1\rho}(H)$ relaxation is sensitive to modulated frequency in the tens of kHz range. The likely molecular motions in this frequency range are those due to the pendent groups of P4VP and PVPh. Since strong inter-molecular hydrogen bonding hinders the motion of the pendent groups, the $T_{1\rho}(H)$ is longer for the blends [17,34,35]. These imply that all the blends are homogeneous on the $T_{1\rho}(H)$ sensitive scale.

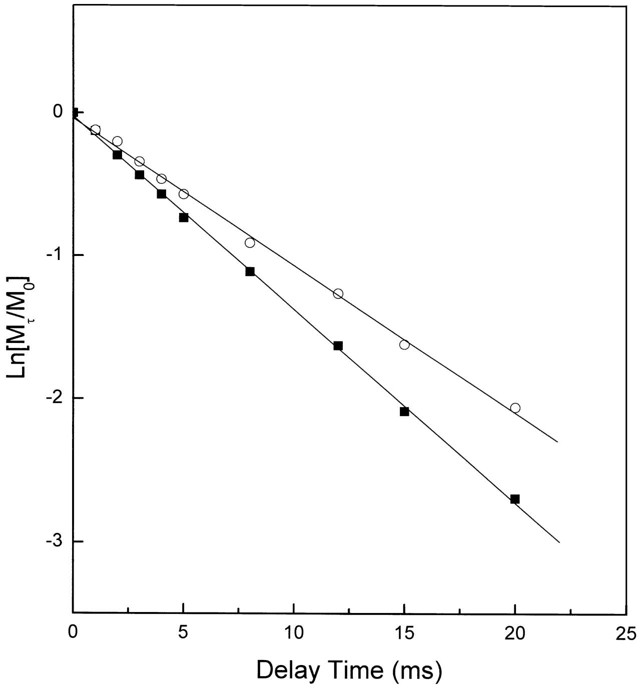

Fig. 6. Logarithmic plot of the peak intensities vs. delay time of $T_{1\rho}(H)$ for the selected carbons of PVPh (C-3). (■) PVPh (○) P4VP/PVPh 50/50.

4. Conclusions

The $T_1(H)$ results are in a good agreement with the thermal analysis and the FTIR result. The results of $T_{1\rho}(H)$ further indicated that the blends ware homogeneous on an even smaller scale. The strong hydrogen bonding between P4VP and PVPh restricts the mobility of the polymer chains as shown by the longer $T_{1\rho}(H)$ values of the blends than those of the pure components.

Acknowledgements

Partial financial support of the grant, RGC HKUST 6120/99P, is acknowledged.

References

[1] Srinivasan D, Natarajan TS, Rangarajan G, Bhat SV, Wessling B. Solid State Commun 1999;110:503–8.
[2] Baik DH, Kim GL, Park YH, Lee YK, Son YK. Polym Bull (Berlin) 1998;41:713–9.
[3] Olabisi O, Robeson LM, Shaw MT. Polymer–polymer miscibility. New York: Academic Press, 1979.
[4] Shaw MT, Walsh DJ, Higgins JS, Maconnachie A, editors. Polymer blends and mixtures. NATO, Advanced Study Institute Series E89. Boston, MA: Martinus Nijhoff, 1985.
[5] Walsh DJ, Rostami S. Adv Polym Sci 1985;70:119.
[6] Ultracki LA. Polymer alloy and blends. Munich: Hanser, 1989.
[7] Kaplan DS. J Appl Polym Sci 1976;20:2615.
[8] McBrierty VJ, Packer KJ. Nuclear magnetic resonance in solid polymer. Cambridge, UK: Cambridge University Press, 1993.

[9] Mathias LJ, editor. Solid state NMR of polymer. New York: Plenum Press, 1991.

[10] Zhang X, Takegoshi K, Hikichi K. Polymer 1992;33:712.

[11] Qin C, Priesm ATN, Belfiore LA. Polym Commun 1990;31:177.

[12] Miyoshi T, Takegoshi K, Hikichi K. Polymer 1997;38:2315.

[13] Zheng S, Guo Q, Mi Y. J Polym Sci, Part B: Polym Phys 1998;36:2291–300.

[14] Zhong Z, Guo Q, Mi QY. Polymer 1998;40:27–33.

[15] Cheung MK, Zheng S, Mi Y, Guo Q. Polymer 1998;39:6289–92.

[16] Zhong Z, Zheng S, Mi Y. Polymer 1999;40:3829–34.

[17] Lau C, Zheng S, Zhong Z, Mi Y. Macromolecules 1998;31:7291–7.

[18] Zhong Z, Mi Y. J Polym Sci, Part B: Polym Phys 1999;37:237–45.

[19] Coleman MM, Lichkus AM, Painter PC. Macromolecules 1989;22:211.

[20] Goh SH, Siow KS. Polym Bull 1987;17:453.

[21] Hong J, Goh SH, Lee SY, Siow KS. Polymer 1995;36:143.

[22] Iriondo P, Iruin JJ, Fernandez-Berridi MJ. Polymer 1995;36:3235.

[23] Iriondo P, Iruin JJ, Fernandez-Berridi MJ. Macromolecules 1996;29:5605.

[24] Belfiore LA, Qin C, Ueda E, Pires ATN. J Polym Sci, Part B: Polym Phys 1993;31:409.

[25] de Meftahi MV, Fréchet JMJ. Polymer 1988;29:477.

[26] Wang LF, Pearce EM, Kwei TK. J Polym Sci, Part B: Polym Phys 1991;29:619.

[27] Meaurio E, Velada JL, Ceateros LC, Katime I. Macromolecules 1996;29:4598.

[28] Zhang X, Takegoshi K, Hikichi K. Macromolecules 1991;24:5756.

[29] White JL, Mirau PA. Macromolecules 1994;27:1648.

[30] Matsuki K, Toshiyuki U, Asakura T. NMR spectroscopy and stereoregularity of polymers. Tokyo/Basel: Japan Scientific Societies Press/S Karger AG, 1996 (p. 170).

[31] McBrierty VJ, Douglass DC. J Polym Sci Macromol Rev 1981;16:295.

[32] Demco DE, Johansson A, Tegenfeldt. J Solid State Nucl Magn Reson 1995;4:13.

[33] Clauss J, Schmidt-Rohr K, Spiess HW. Acta Polym 1993;44:1.

[34] Jack KS, Whittaker AK. Macromolecules 1997;30:3560.

[35] VanderHart DL, Garroway AN. J Chem Phys 1979;71:2773.